Optical Engineering

OpticalEngineering.SPIEDigitalLibrary.org

Single-mode interband cascade laser multiemitter structure for two-wavelength absorption spectroscopy

Julian Scheuermann
Robert Weih
Steffen Becker
Marc Fischer
Johannes Koeth
Sven Höfling

SPIE.

Julian Scheuermann, Robert Weih, Steffen Becker, Marc Fischer, Johannes Koeth, Sven Höfling, "Single-mode interband cascade laser multiemitter structure for two-wavelength absorption spectroscopy," *Opt. Eng.* **57**(1), 011008 (2017), doi: 10.1117/1.OE.57.1.011008.

Single-mode interband cascade laser multiemitter structure for two-wavelength absorption spectroscopy

Julian Scheuermann,[a,*] Robert Weih,[a,b] Steffen Becker,[a] Marc Fischer,[a] Johannes Koeth,[a] and Sven Höfling[b,c]
[a]nanoplus Nanosystems and Technologies GmbH, Gerbrunn, Germany
[b]Universität Würzburg, Technische Physik and Wilhelm Conrad Röntgen Research Center for Complex Material Systems, Würzburg, Germany
[c]University of St. Andrews, Scottish Universities Physics Alliance, School of Physics and Astronomy, St. Andrews, United Kingdom

Abstract. An interband cascade laser multiemitter with single-mode distributed feedback (DFB) emission at two wavelengths is presented. Continuous-wave laser operation is measured from 0°C to 40°C with threshold currents of around 25 mA and output powers of around 9 mW at 20°C. The ridge waveguide DFB structures are monolithically integrated with a spacing of 70 μm and each is provided with an individual metal DFB grating to select specific single-mode wavelengths of interest for absorption spectroscopy. The emission windows at 3.92 and 4.01 μm are targeting hydrogen sulfide and sulfur dioxide, which are of importance for industrial applications since both gases are reagents of the Claus process in sulfur recovery units, recovering elemental sulfur from gaseous hydrogen sulfide. [DOI: 10.1117/1.OE.57.1.011008]

Keywords: interband cascade laser; distributed feedback; absorption spectroscopy; laser spectroscopy; infrared spectroscopy; process control.

Paper 170835SS received Jun. 2, 2017; accepted for publication Aug. 16, 2017; published online Sep. 11, 2017.

1 Introduction

1.1 *Interband Cascade Laser*

Interband cascade laser (ICL) technology has gotten more and more mature and versatile since it was proposed more than two decades ago.[1] The performance characteristics increased significantly, both with respect to high temperature operation and output power. A key element of this advance was the carrier rebalancing concept[2] enabling ICL devices in a wide wavelength window to operate in continuous-wave (cw) mode at room temperature and above. By optimizing the active region design and the number of active stages, output powers in the range of hundreds of milliwatts were achieved.[3,4]

In addition, various schemes for distributed feedback (DFB) were investigated by now. Top-gratings, as well known from quantum cascade laser (QCL) technology, can also be used for ICLs. Single-mode laser emission was demonstrated using a Ge top-grating in an overgrowth-free processing route[5] and respective devices were operated in cw mode up to 80°C. Similar approaches using intrinsic semiconductor material instead of germanium gratings are vertical sidewall gratings[6] and grating structures implemented by a two-step ridge waveguide etch process.[7] Another technique using lateral metal grating structures at the side of the ridge waveguide was also recently demonstrated.[8,9] The latter approach was also pursued for the device concept as presented in this work.

1.2 *Spectroscopy*

Nowadays, ICLs can be found in a variety of applications, benefitting from the possibility of low power cw operation at room temperature and above.[10]

Tunable laser absorption spectroscopy (TLAS) has been a very common technique used in gas-sensing applications for many years. While Fabry–Pérot type ICL devices can be used for measurements of multiple gas species or broad signatures of complex molecules,[11] for applications targeting high sensitivity and low detection limits, single-mode DFB ICL devices are typically used.

Starting based on single-mode diode lasers in the near-infrared, the technological progress of midinfrared (MIR) semiconductor laser sources, such as QCLs and ICLs, has made this wavelength range accessible for new and improved applications. The advantage for spectroscopic applications is based on order of magnitudes higher absorption strength of the fundamental lines located in the MIR region. In an optical measurement, some gases such as sulfur dioxide can be exclusively addressed in the MIR (Fig. 1).

1.3 *Application*

The Claus process is the most significant gas desulfurizing process. The multistep process recovers sulfur from the gaseous hydrogen sulfide found in raw natural gas and from the by-product gases containing hydrogen sulfide derived from refining crude oil and other industrial processes. Since hydrogen sulfide is highly toxic and harmful to the environment, the H_2S has to be removed from the base product and is fed into sulfur recovery units, using the Claus process [Eq. (1)] for generating elemental sulfur. The Claus reaction that converts H_2S into elemental sulfur requires the presence of one mole SO_2 for each of the two moles of H_2S. Therefore, the correct ratio of components is generated in a first combustion step [Eq. (2)] converting one-third of the H_2S in the fed gas.

$$2H_2S + SO_2 \rightarrow 3S + 2H_2O, \quad (1)$$

*Address all correspondence to: Julian Scheuermann, E-mail: julian.scheuermann@nanoplus.com

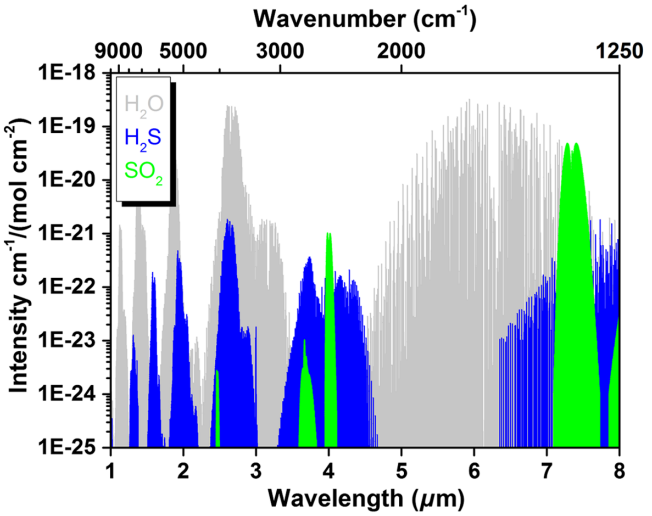

Fig. 1 Overview of the intensity of the absorption lines of water, hydrogen sulfide, and sulfur dioxide-based on the HITRAN database. In an optical measurement, sulfur dioxide can be detected exclusively in the MIR. The wavelength region around 4 μm has both low interfering water absorption lines as well as high absorption line strength for hydrogen sulfide and sulfur dioxide.

$$H_2S + 1.5O_2 \rightarrow SO_2 + H_2O. \quad (2)$$

As a result, the combination of Eqs. (1) and (2) is

$$2H_2S + O_2 \rightarrow 2S + 2H_2O. \quad (3)$$

For a successful process control application, measuring SO_2 and H_2S is essential. For TLAS application and a real-time control system, the wavelength region around 4 μm is ideally suited, since it has low interfering water absorption lines and suitable absorption line strength for SO_2 and H_2S.

2 ICL-Based Material Growth and Device Processing

The IC laser structure was grown by solid source molecular beam epitaxy as described in Ref. 12, with the following minor optimizations to the design: the layer structure of the six stage active region and the injector structures were adjusted with respect to the emission wavelength. The W-type quantum well (W-QW) layer sequence comprises AlSb/InAs/$Ga_{0.65}In_{0.35}$Sb/InAs/AlSb of thicknesses 2.50/1.97/3.00/1.56/1.00 nm. In doing so, the thickness of the InAs layers was adjusted with respect to the emission wavelength of around 3.9 μm at room temperature, ideal for DFB detuning and performance at both targeted wavelength channels. The electron injector region contained five InAs/AlSb pairs, where the four InAs wells closest to the W-QW were highly Si-doped with 6×10^{18} cm^{-3} for carrier rebalancing.[2] For optical confinement, the active region was enclosed in 360-nm-thick GaSb separate confinement layers as well as an upper and lower AlSb/InAs superlattice cladding structures with a thickness of 1.8 and 3.1 μm, respectively. In addition, specific growth techniques were implemented such as transition layers to smoothen out conduction band discontinuities and graded cladding layer doping concentration for reduced optical absorption. Broad area (BA) devices were fabricated to investigate the basic IC laser material

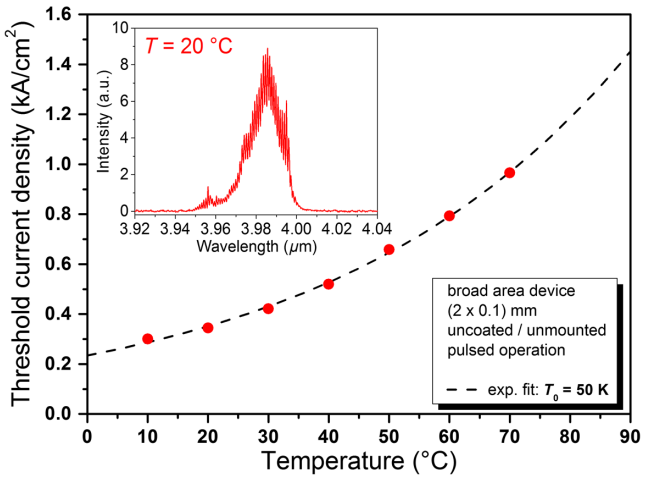

Fig. 2 Threshold current density of a shallowly etched broad area device as a function of temperature. A characteristic temperature of 50 K was derived from the exponential curve fitting. The uncoated and unmounted BA device with dimensions of 2 mm $\times$ 100 μm was operated in pulsed mode. The inset shows the respective emission spectrum at 20°C and an injection current density of 0.45 kA/cm^2.

performance. The BA lasers with ridge waveguide dimensions of 2 mm $\times$ 100 μm were shallowly etched to a depth of around 1.5 μm. A threshold current density (J_{th}) of 0.35 kA/cm^2 was measured in pulsed operation at 20°C and a characteristic temperature of 50 K was derived from temperature-dependent measurements of J_{th} (Fig. 2). The inset shows an emission spectrum with a pulsed driving current density of 0.45 kA/cm^2.

Narrow ridge waveguide structures were fabricated as described in Ref. 9 whereas the width of the ridge was increased to 6.5 μm. The developed chip design is using two ridge waveguide structures with 70 μm spacing and separated electrical contacts with total chip dimensions of 900 μm $\times$ 350 μm. The samples were cleaved into 900-μm long bars and coated with a metal-based high reflectivity mirror on the back and a 30-nm Al_2O_3 layer on the front facet. Single dies were soldered on AlN heat spreaders and subsequently mounted on TO-style headers. The headers were sealed under dry air atmosphere using a steel cap with

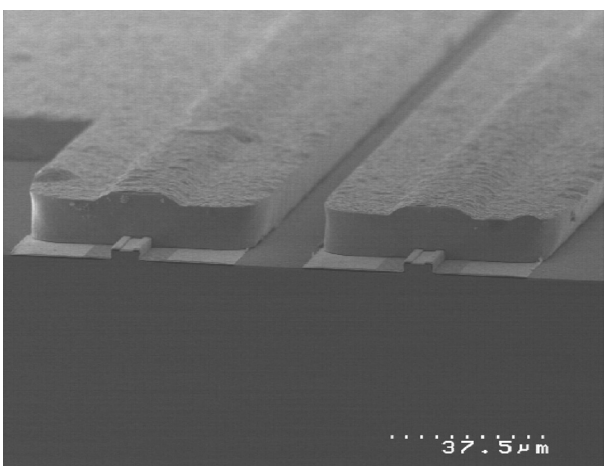

Fig. 3 Scanning electron micrograph of the cleaved laser facet. The individual waveguides of the two DFB emitters with the respective top contact metallization and the electroplated gold contacts are shown.

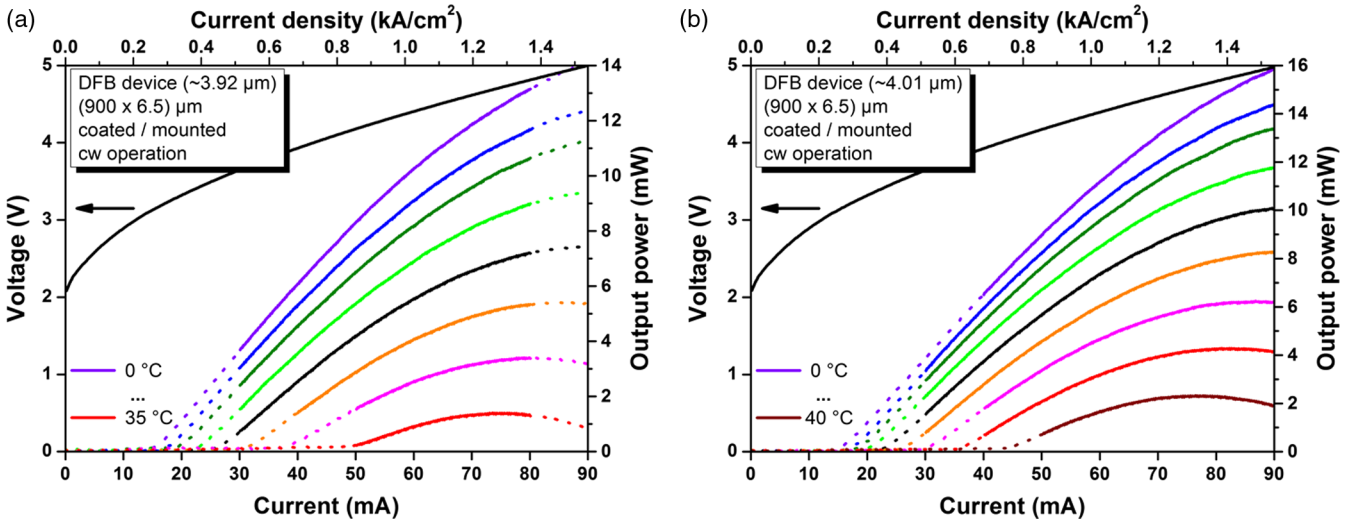

Fig. 4 Temperature-dependent $L-I-V$ characteristics of two DFB emitters based on the developed chip design with emission windows at (a) 3.92 and (b) 4.01 μm, respectively. The solid lines depict single-mode operation with setup limited SNR of more than 25 dB. The facet-coated laser chips with ridge waveguide dimensions of 900 μm $\times$ 6.5 μm were mounted on a TO-style header.

AR-coated window. Figure 3 shows a scanning electron micrograph of the cleaved laser facets. The individual waveguides of the two DFB emitters with the respective top contact metallization and the electroplated gold contacts are observed.

3 Results and Application Example

Temperature-dependent $L-I-V$ characteristics for two adjacent DFB emitters are shown in Fig. 4. The solid lines represent single-mode emission with setup limited signal-to-noise ratio (SNR) of more than 25 dB (spectra not shown), and the dashed lines represent emission with lower SNR (near threshold) or multiple mode operation. The ICL-based device shows application-grade DFB performance characteristics with laser emission measured from 0°C to 40°C, threshold currents around 25 mA and single-mode output powers of around 9 mW at 20°C. The approximate gain position of the underlying IC material can be derived from the Fabry–Pérot spectrum shown in the inset of Fig. 2 as measured in pulsed mode at an operation temperature of 20°C. Due to joule heating in cw mode, the spectral gain position is shifted toward higher wavelengths. Especially at increased operation temperatures this leads to a stronger decrease in performance for the 3.92-μm wavelength channel as compared to the 4.01 μm channel and results in a lower maximum operation temperature as can be observed from the $L-I-V$ curves shown in Fig. 4. For an operation temperature of 20°C, the two emission windows at 3.92 and 4.01 μm with a tuning range of 7 and 8 nm, respectively, will make spectroscopic measurements of both hydrogen sulfide and sulfur dioxide possible. Figure 5 shows two tuning diagrams for each channel of the multiemitter

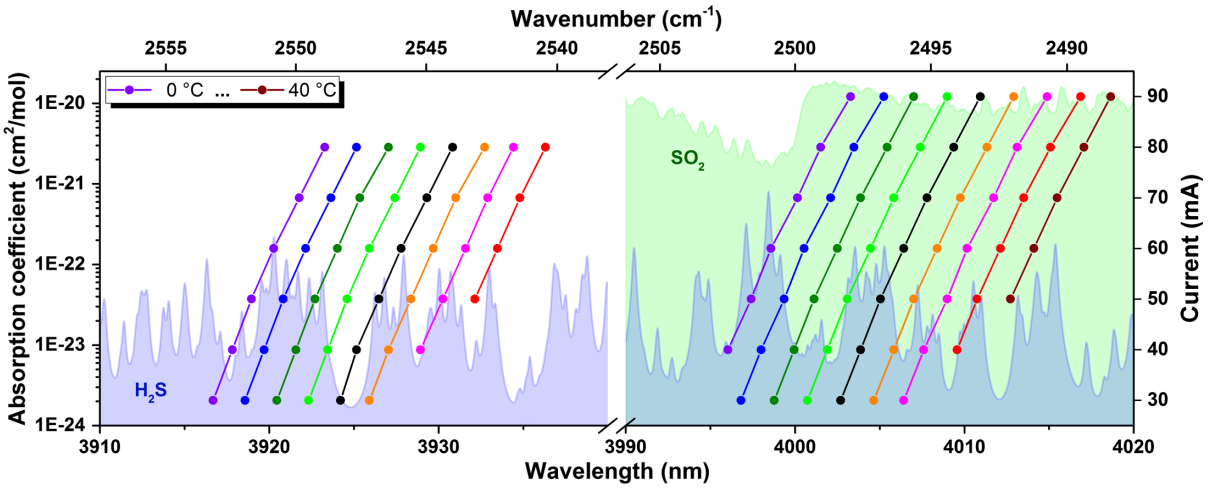

Fig. 5 Two tuning diagrams for the individual DFB emitters of the multiemitter structure. The circles show the single-mode DFB emission wavelengths for different driving currents and temperatures. Also shown is the wavelength-dependent absorption coefficient (at SATP) for both hydrogen sulfide (blue) and sulfur dioxide (green).

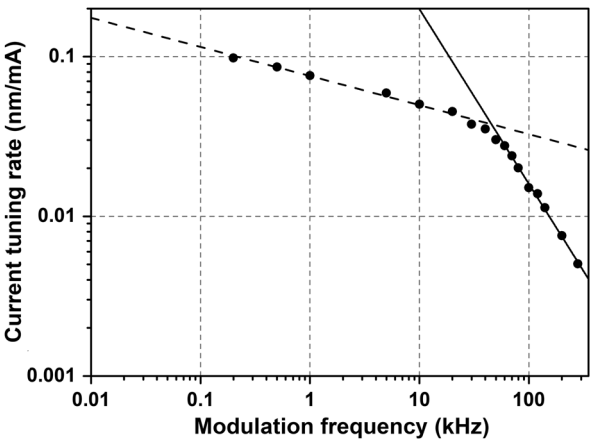

Fig. 6 Frequency-dependent current tuning rate measured by analyzing traces of a 1-in. Ge etalon. For modulation frequencies in the range up to around 30 kHz, the tuning rate decreases with a factor of 0.66 per decade (the dashed line in the graph shows a corresponding curve fit). For higher modulation frequencies above around 30 kHz, the tuning rate decreases with a factor of 0.08 per decade (solid fit line).

structure with a temperature tuning rate of 0.38 nm/K and respective tuning rates of 0.14 nm/mA (25 nm/W) for the current (electrical power)-dependent tuning. The circles show single-mode DFB emission wavelengths for different driving currents and temperatures. Also shown is the wavelength-dependent absorption coefficient at standard ambient temperature and pressure (SATP) for both hydrogen sulfide (blue) and sulfur dioxide (green).[13] Based on the tuning rates, a thermal resistance of 64 K/W was calculated for both waveguides. We also investigated thermal crosstalk by measuring a drive power-induced wavelength shift of 4.5 nm/W between the neighboring lasers, which corresponds to a thermal resistance of 11 K/W. The DFB emission wavelength tuning is caused by joule heating. This thermal effect is strongly dependent on the modulation frequency of the drive current. The relative DFB wavelength tuning was measured for various modulation frequencies by analyzing traces of a 1-in. Ge etalon, which is shown in Fig. 6. Typically, for a $2f$ wavelength modulation spectroscopy setup, lower frequencies in the range from 0.1 to 10 kHz are used for emission wavelength tuning, whereas higher frequencies up to a few tens of kHz can be superimposed for enhanced data acquisition.[14] For modulation frequencies up to around 30 kHz, the current tuning rate drops with a factor of 0.66 per decade (dashed line). For higher frequencies, the rate then drops significantly with a factor of 0.08 per decade (solid line).

4 Conclusion

In conclusion, we presented a DFB multiemitter structure based on two monolithically integrated single-mode ICLs with a ridge waveguide spacing of 70 μm for (simultaneous) spectroscopic measurements of hydrogen sulfide (emission wavelength at around 3.92 μm) and sulfur dioxide (emission wavelength at around 4.01 μm). The device operates in cw mode up to 40°C with threshold currents of around 25 mA and an output power of around 9 mW at 20°C.

The demonstrated multiemitter concept is, in principle, expandable to more waveguides and wavelengths. However, the following challenges have to be considered depending on the exact application requirements: the response time for the measurement will be increasing when using a time-multiplexing procedure for controlling the individual channels. In contrast, when using a frequency-multiplexing procedure, the requirements concerning data acquisition and evaluation will become more complex.

References

1. R. Q. Yang, "Infrared laser based on intersubband transitions in quantum wells," *Superlattices Microstruct.* **17**(1), 77–83 (1995).
2. I. Vurgaftman et al., "Rebalancing of internally generated carriers for mid-infrared interband cascade lasers with very low power consumption," *Nat. Commun.* **2**, 585 (2011).
3. M. Kim et al., "High-power continuous-wave interband cascade lasers with 10 active stages," *Opt. Express* **23**(8), 9664–9672 (2015).
4. I. Vurgaftman et al., "Interband cascade lasers," *J. Phys. D* **48**, 123001 (2015).
5. C. S. Kim et al., "Mid-infrared distributed-feedback interband cascade lasers with continuous-wave single-mode emission to 80°C," *Appl. Phys. Lett.* **101**, 061104 (2012).
6. M. von Edlinger et al., "Monomode interband cascade lasers at 5.2 μm for nitric oxide sensing," *IEEE Photonics Technol. Lett.* **26**(5), 480–482 (2014).
7. S. Forouhar et al., "Reliable mid-infrared laterally-coupled distributed-feedback interband cascade lasers," *Appl. Phys. Lett.* **105**, 051110 (2014).
8. R. Weih et al., "Single mode interband cascade lasers based on lateral metal gratings," *Appl. Phys. Lett.* **105**, 071111 (2014).
9. J. Scheuermann et al., "Single-mode interband cascade lasers emitting below 2.8 μm," *Appl. Phys. Lett.* **106**, 161103 (2015).
10. L. Dong et al., "Compact CH_4 sensor system based on a continuous-wave, low power consumption, room temperature interband cascade laser," *Appl. Phys. Lett.* **108**, 011106 (2016).
11. J. H. Northern et al., "Mid-infrared multi-mode absorption spectroscopy using interband cascade lasers for multi-species sensing," *Opt. Lett.* **40**(17), 4186–4189 (2015).
12. R. Weih, M. Kamp, and S. Höfling, "Interband cascade lasers with room temperature threshold current densities below 100 A/cm^2," *Appl. Phys. Lett.* **102**, 231123 (2013).
13. R. V. Kochanov et al., "HITRAN application programming interface (HAPI): a comprehensive approach to working with spectroscopic data," *J. Quant. Spectrosc. Radiat. Transfer* **177**, 15–30 (2016).
14. L. Dong et al., "Ppb-level formaldehyde detection using a CW room-temperature interband cascade laser and a miniature dense pattern multipass gas cell," *Opt. Express* **23**(15), 19821–19830 (2015).

Julian Scheuermann received his Dipl Ing degree in nanotechnology engineering from the University of Würzburg, Germany, in 2012. He then joined nanoplus Nanosystems and Technologies GmbH and is now working in the R&D division on advanced laser sources for spectroscopic applications. His research interests are in the area of innovative MID-IR interband cascade-based light sources.

Robert Weih received his Dipl Ing degree in nanotechnology engineering from the University of Würzburg, Germany, in 2011. In 2015, he joined the epitaxy division at nanoplus Nanosystems and Technologies GmbH, an ISO 9001 and 14001 certified supplier of semiconductor devices and lasers for trace gas sensing. His research interests are in the area of molecular beam epitaxy for innovative MID-IR laser and detector structures.

Steffen Becker received his BEng degree in laser technology/optoelectronic from the University of Applied Science Aalen, Germany, in 2013, and his MSc degree in photonics from the University of Jena, Germany, in 2015. He joined the R&D division at nanoplus Nanosystems and Technologies GmbH in the same year, where he is working on advanced sources for laser spectroscopy. His research interests are in the area of MID-IR interband cascade laser sources and their applications.

Marc Fischer received his master's degree in 1997 from the State University of New York at Buffalo as well as his Dipl Phys and PhD degree from the University of Würzburg in 1999 and 2003, respectively, all in physics. In 2002, he joined nanoplus Nanosystems and Technologies GmbH, where he is currently managing the

R&D division. His research interest has been in the area of innovative semiconductor material and devices in the near-infrared and MID-IR.

Johannes Koeth received his Dipl Phys and PhD degree from the University of Würzburg in 1996 and 2002, respectively, all in physics. In 1998, he cofounded nanoplus Nanosystems and Technologies GmbH and has been the CEO of the company ever since. His research interests have been in the area of molecular beam epitaxy and innovative semiconductor laser structures. He authored around 150 publications of innovative semiconductor devices and their applications in sensing.

Sven Höfling received his Diploma in applied physics from the University of Applied Science Coburg, Germany. In 2003, he joined the Department Technische Physik, Universität Würzburg, Germany, for his PhD work on single-mode emitting quantum cascade lasers. He is a professor in physics and holds a personal chair at Würzburg University, Germany, and the University of St. Andrews, Scotland, since 2015 and 2013, respectively. His research is concerned with the design, fabrication, and characterization of low-dimensional electronic and photonic structures.